Supplementary Material

Dynamic beam shifting via refractive index tuning

Authors: *Mingxuan Gu[1,2†], Xinghong Chen[1†], Yifei Mao[1,2*]*

Affiliations:

[1]School of Sensing Science and Engineering, School of Electronic Information and Electrical Engineering, Shanghai Jiao Tong University, Shanghai 200240, China.

[2]SJTU-Pinghu Institute of Intelligent Optoelectronics, Pinghu 314200, China.

[*]Correspondence to: maoyifei@sjtu.edu.cn;

Outline

Section 1. Basic principle based on coupled-mode theory

Coupled-mode theory (CMT) can be used to describe the interaction between an optical resonator and m ports, hence, it can also describe the responses between external fields and optical modes supported by a PhC cavity. We consider an incidence with a certain in-plane $k_{||}$, the scattering process can be expressed as:

$$|E_{out}\rangle = \begin{bmatrix} s_u \\ s_d \end{bmatrix}_- = \mathrm{S} \begin{bmatrix} s_u \\ s_d \end{bmatrix}_+ = \mathrm{S}|E_{in}\rangle \tag{S1}$$

Here, $s_{u\pm}$ ($s_{d\pm}$) represent the incoming/outgoing beams of the upper (down) side of the PhC resonator, S is referred to the scattering matrix. Now we consider the radiative modes of the PhC slab with C_{4v} symmetry. Note that the states of polarization (SOPs) of the modes around bound states in the continuum (BICs) are nearly linearly polarized, the CMT incorporating $k_{||} - r_{||}$ can be expressed as:

$$\frac{dA}{d\boldsymbol{r}_{||}} = \left(ik_0 - \alpha_{v_g} \sum \gamma_m\right) A + \alpha_{v_g} K^T |s_+\rangle,\ \alpha_{v_g} = sgn(v_g)$$

$$|s_-\rangle = C|s_+\rangle + DA = \mathbb{S}|s_+\rangle. \tag{S2}$$

Here, A represents the field amplitude of the resonance, and $\boldsymbol{r}_{||}$ is the in-plane position, whose direction is parallel to $k_{||}$. The parameter α_{v_g} denotes the group velocity factor of the radiative mode, and γ_m refers to the radiation loss of m-th port. Additionally, k_0 is the wave vector of the resonant radiative mode along the same direction as $k_{||}$. The matrix C is the generalized background scattering matrix, and K, D are the coupling coefficients between the resonance and the ingoing and outgoing plane waves. By considering the resonance of in-plane $k_{||}$, we can solve Equation S2 for the scattering matrix S:

$$\mathrm{S} = C + \frac{DK^T}{i\alpha_{v_g}(|k_{||}| - k_0) + \sum \gamma_m} \tag{S3}$$

In our work, we focus on the incidence along the Γ-X direction. In this direction, s/p-polarization corresponds to y/x-polarization, the SOPs of the radiative modes are either x-polarized or y-polarized due to mirror symmetry. Now we assume that the SOPs are x-polarized, as the conclusions remains the same for the y-polarized case. Under the x-y polarization basis, these parameters can be expressed as:

$$|s_+\rangle = \begin{bmatrix} E_u^x \\ E_d^x \\ E_u^y \\ E_d^y \end{bmatrix}_+ , \ |s_-\rangle = \begin{bmatrix} E_u^x \\ E_d^x \\ E_u^y \\ E_d^y \end{bmatrix}_- ,$$

$$C = \begin{bmatrix} r_x & t_x & 0 & 0 \\ t_x & r_x & 0 & 0 \\ 0 & 0 & r_y & t_y \\ 0 & 0 & t_y & r_y \end{bmatrix}, \ K = \begin{bmatrix} k_x \\ \alpha_z k_x \\ 0 \\ 0 \end{bmatrix}, \ D = \begin{bmatrix} d_x \\ \alpha_z d_x \\ 0 \\ 0 \end{bmatrix}. \quad \text{(S4)}$$

Here, r_x/r_y and t_x/t_y represent the background reflection and transmission coefficients for x/y polarization. The parameter α_z is a parity number that links the upward and the downward radiation due to the sample-plane mirror symmetry. (α_z = ±1, +1 and −1 correspond to even and odd symmetry, respectively). Considering the conditions of energy conservation and the space-reversal process condition of the system, we obtain constraints on the scattering matrix and coupling coefficients in Equation S2 as:

$$D^\dagger D = 2\sum\gamma_m, \ K = D, \ CD^* = -D. \quad \text{(S5)}$$

Here, $\sum\gamma_m = \gamma_u^x + \gamma_d^x = 2\gamma$. And using equation S5, we obtain:

$$\left|d_y\right| = \sqrt{2\gamma}, \ (r_x + \alpha_z t_x)d_x^* = -d_x. \quad \text{(S6)}$$

Now we consider the incidence only from the upper side, that is, $|s_+\rangle = [E_u^x \quad 0 \quad E_u^y \quad 0]_+^T$, using Equations S3, S5 and S6, the reflection matrix $\mathbb{R}$ can be written as:

$$|r\rangle = \begin{bmatrix} E_u^x \\ E_u^y \end{bmatrix}_- = \mathbb{R}\begin{bmatrix} E_u^x \\ E_u^y \end{bmatrix}_+$$

$$\mathrm{R} = \begin{bmatrix} r_x + \frac{d_x^2}{i\alpha_{v_g}(|k_{||}|-k_0)+2\gamma} & 0 \\ 0 & r_y \end{bmatrix} \quad \text{(S7)}$$

In our design, to excite the Γ-BIC mode, the incidence is nearly normal. Under this condition, we have the approximation $r_x = r_y = |r|e^{i\varphi_r}, \ t_x = t_y = |t|e^{i\varphi_t}$. The reflection matrix R can then be further expressed as:

$$\mathrm{R} = \begin{bmatrix} -\frac{\alpha_{v_g}|r|(|k_{||}|-k_0)+2\alpha_z\gamma|t|}{i\alpha_{v_g}(|k_{||}|-k_0)+2\gamma}e^{i\varphi_t} & 0 \\ 0 & |r|e^{i\varphi_r} \end{bmatrix} = \begin{bmatrix} r_{xx} & 0 \\ 0 & r_{yy} \end{bmatrix}, \quad \text{(S8)}$$

$$R_{xx} = |r_{xx}|^2 = \frac{[\alpha_{v_g}|r|(|k_{||}|-k_0)+2\alpha_z\gamma|t|]^2}{4\gamma^2+(|k_{||}|-k_0)^2}. \quad \text{(S9)}$$

Here, R_{xx} represents the reflectance under x-polarized incidence. Based on the assumption that the SOP of the resonant mode is y-polarized, we can generalize the

results to SOPs with an arbitrary orientation. To achieve this, we select an orientation with an azimuthal angle θ as the x' direction, defining a new coordinate system $\widehat{x'} - \widehat{y'}$. Using the concept of coordinate basis rotation, the reflection matrix $\mathrm{R}(\theta)$ in this direction can be represented as $\mathrm{R}(\theta) = R^{-1}(\theta) \cdot \mathrm{R} \cdot R(\theta)$, where the rotation matrix is defined as:

$$R(\theta) = \begin{bmatrix} cos\theta & sin\theta \\ -sin\theta & cos\theta \end{bmatrix}. \tag{S10}$$

Next, we consider the condition under the left circularly polarized (LCP) and right circularly polarized (RCP) basis. We define the x-polarized and y-polarized unit vectors as $|X\rangle = (1,0)^T$, $|Y\rangle = (0,1)^T$, the LCP and RCP unit vectors can then be defined as $|L\rangle = \frac{1}{\sqrt{2}}(1,\ i)^T$ and $|R\rangle = \frac{1}{\sqrt{2}}(1,\ -i)^T$. Notice that the definitions of LCP and RCP are consistent with those in which the incident propagation direction $\boldsymbol{k}$ is chosen as the $\hat{z}$ direction of the right-handed coordinate system. The transformation matrix T that converts the linearly polarized basis (X, Y) to the helical basis (L, R) can be expressed as:

$$T = \frac{1}{\sqrt{2}}\begin{bmatrix} 1 & 1 \\ -i & i \end{bmatrix}. \tag{S11}$$

Then the reflection matrix S can be written as:

$$\begin{aligned} \mathrm{S} = T^{-1}\mathrm{R}(\theta)T &= T^{-1}R^{-1}(\theta) \cdot \mathrm{R} \cdot R(\theta)T \\ &= \frac{1}{2}\begin{bmatrix} r_{xx} + r_{yy} & (r_{xx} - r_{yy})e^{i2\theta} \\ (r_{xx} - r_{yy})e^{-i2\theta} & r_{xx} + r_{yy} \end{bmatrix} \\ &= \begin{bmatrix} r_{ll} & r_{lr}e^{i2\theta} \\ r_{rl}e^{-i2\theta} & r_{rr} \end{bmatrix}. \end{aligned} \tag{S12}$$

For the helical basis, the LCP and RCP unit vectors are defined as $|L\rangle = (1,0)^T$, $|R\rangle = (0,1)^T$. $r_{ll}, r_{lr}, r_{rl}, r_{rr}$ are reflection coefficients of the resonance. The off-diagonal elements of matrix S include additional geometric phase factors $e^{\pm i2\theta}$, known as the Pancharatnam-Berry (PB) phase. PB phase arises due to the coupling between the spin of light and the coordinate frame rotations in momentum space, revealing the extrinsic spin-orbit interaction (SOI) of light induced by mode resonances.

When the incidence is LCP, the output can be determined using the reflection matrix S as:

$$|E_{out}\rangle = r_{rl}e^{-i2\theta}\langle L|E_{in}\rangle|R\rangle + r_{ll}\langle L|E_{in}\rangle|L\rangle. \tag{S13}$$

In Equation S13, $r_{rl}e^{-i2\theta}\langle L|E_{in}\rangle|R\rangle$ is the cross-polarization part, and the reflection phase can be deduced as:

$$\varphi_{lr}(\boldsymbol{k}_{||}) = angle(r_{rl}) - 2\theta \tag{S14}$$

We can now identify the cross-polarization phase (the first term) and PB phase (the second term) in Equation S14, as previously discussed for the reflection matrix S (Equation S12). For the Γ-BIC, the SOPs remain the same along the Γ-X direction, by using Equation S8 and S12, the cross-polarized (RCP) phase gradients under incidence along the Γ-X direction can be written as:

$$\frac{\partial \varphi_{lr}(\boldsymbol{k}_{||})}{\partial \boldsymbol{k}} = \frac{\partial \varphi_{lr}(\boldsymbol{k}_{||})}{\partial k_x}\hat{x} + \frac{\partial \varphi_{lr}(\boldsymbol{k}_{||})}{\partial k_y}\hat{y} = \frac{2\alpha_{v_g}\gamma}{4\gamma^2+(|\boldsymbol{k}_{||}|-k_0)^2}\hat{\boldsymbol{x}} - \frac{2\partial\theta}{\partial k_y}\hat{\boldsymbol{y}} \tag{S15}$$

As mentioned in the main text, the momentum space and the spatial space form a pair of reciprocal spaces. Spatial beam shifts can be realized through the phase gradient constructed in the momentum space. Specifically, this can be expressed as:

$$\hat{r} = i\frac{\partial}{\partial \boldsymbol{k}},\ \boldsymbol{R} = -\frac{\partial \varphi(\boldsymbol{k}_{||})}{\partial \boldsymbol{k}},$$

$$\boldsymbol{R}_{RCP} = \mathbf{X} + \mathbf{Y} = \frac{2\alpha_{v_g}\gamma}{4\gamma^2+(|\boldsymbol{k}_{||}|-k_0)^2}\hat{\boldsymbol{x}} + \frac{2\partial\theta(\boldsymbol{k}_{||})}{\partial k_y}\hat{\boldsymbol{y}} \tag{S16}$$

Hence, the beam shifts in the Y-direction are determined by PB phase gradients and the spin direction of the incident light. As shown in Fig. S1, when the structure (a = 1100 nm, D = 760 nm, t = 200 nm) is illuminated with an LCP incidence (consist of two orthogonal Gaussian beams with a phase difference of 90° at the center of the slab, the incidence is near normal for better exciting the BIC modes, and the divergence angle is 1.3°), and the refractive index of the structure is set to be 2 (Fig. S1a) and 2.4 (Fig. S1b), modes similar to mode 1 and mode 2 mentioned in the main text will be excited (will be referred to as mode 1 and mode 2 in this part), respectively. The beam shifts of the cross-polarized (RCP) reflected light for mode 1 are -12.63 μm and 5.85 μm in X and Y-direction (Fig. S1a), respectively; the beam shifts of RCP reflected light for mode 2 are 8.65 μm and -5.46 μm in X and Y-direction (Fig. S1a), respectively.

When the structure is illuminated with an RCP incidence under the same condition, the cross-polarized (LCP) reflected light is symmetrical to the previous result about the X-axis (mode 1: x = -12.64 μm, y = -5.86 μm; mode 2: x = 8.65 μm, y = 5.46 μm). The cross-polarization phase gradient contributes to beam shifts in the X-direction, which is determined by group velocity factor α_{v_g}. The value of α_{v_g} can be directly obtained from the band structure.

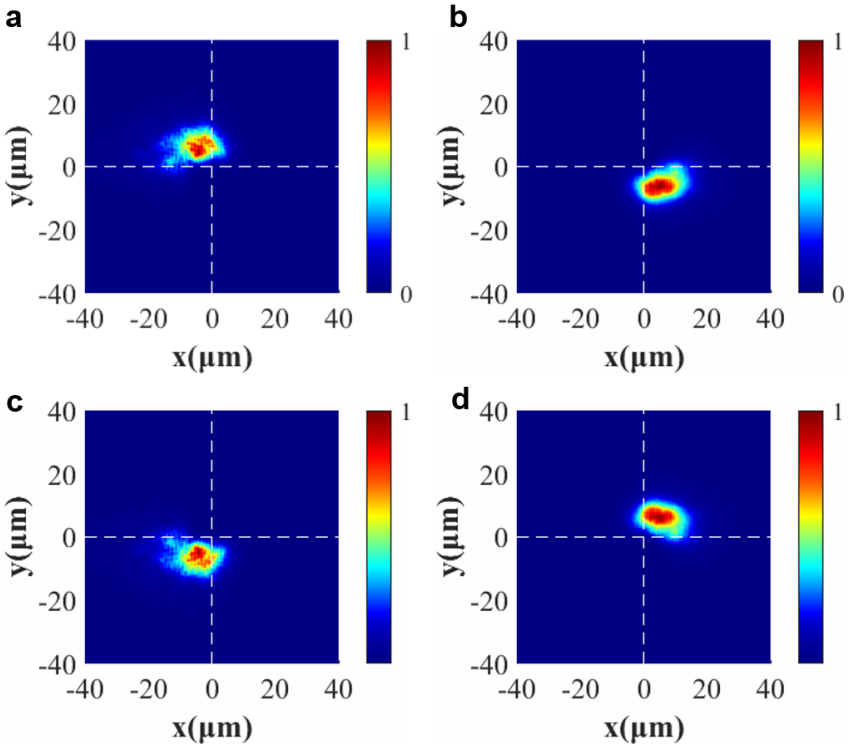

Figure S1. Influence of incident spin direction. The reflective intensity distribution with incidence of LCP (**a**, **b**) or RCP (**c**, **d**). The value of beam shifts is **a**: x = -12.63 μm, y = 5.85 μm; **b**: x = 8.65 μm, y = -5.46 μm; **c**: x = -12.64 μm, y = -8.56 μm; **d**: x = 8.65 μm, y = 5.46 μm.

Section 2. The refractive index of Sb_2Se_3

In main text discussing phase change materials, we demonstrate the feasibility of our design by employing a two-layer structure instead of a single-layer structure. This is because the inherent losses of PCMs will significantly impact the characteristics of our device.

Therefore, we refer to Sb_2Se_3, which exhibits relatively low ohmic loss in the near-infrared range compared to many other phase change materials. The refractive index of Sb_2Se_3 was measured using a dual rotating-compensator Mueller matrix ellipsometer, and the result is shown in Fig. S2. The real part of the refractive index of Sb_2Se_3 in amorphous phase and crystalline phase is represented by red dotted line and red solid line, respectively. These values correspond to the main Y-axis on the left (in red). The imaginary part of the refractive index of Sb_2Se_3 in amorphous phase and crystalline phase is represented by blue dotted line and blue solid line, respectively. These values correspond to the secondary Y-axis on the right (in blue).

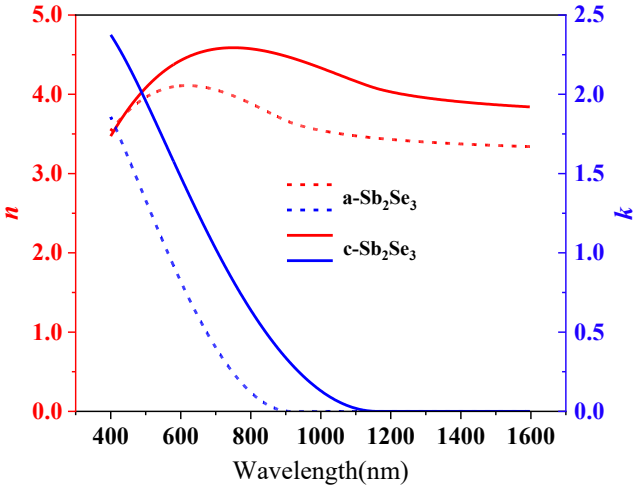

Figure S2. The measured refractive index of Sb2Se3 in both the amorphous and crystalline states. The ohmic loss is relatively low in the near-infrared range.

Section 3. The effect of wavelength changing on beam shifts.

The process of slightly tuning the refractive index of electro-optical materials can be understood as adjusting the position of the band structure relative to the incident wavelength. Conversely, a similar effect can be achieved by directly varying the incident wavelength. Although changing the wavelength of incident light does not qualify as dynamically control under the definition, it provides a practical method for scanning across different angular ranges by selecting appropriate incident wavelengths. Here, we analyze mode 4 as described in the main text (a = 1400 nm, D = 880 nm, t = 300 nm, n = 3.3).

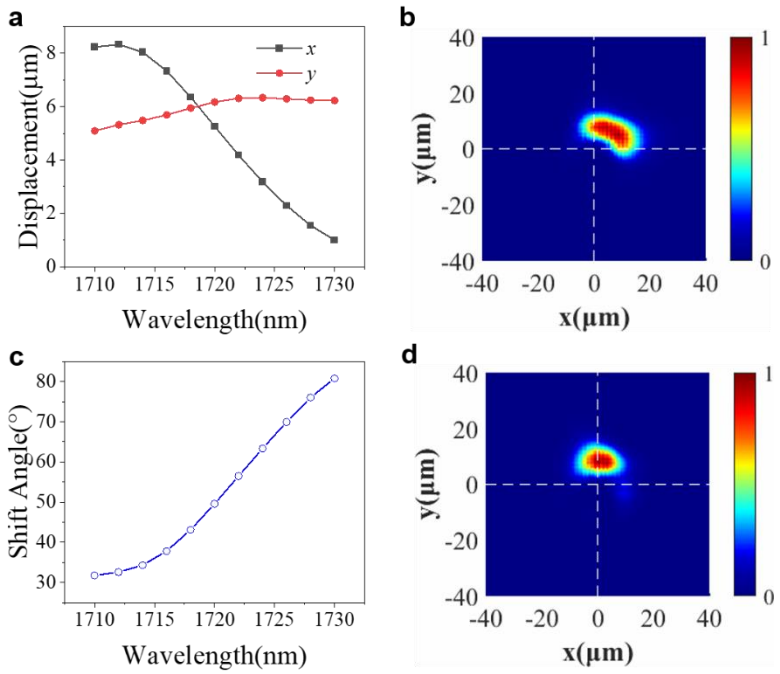

Figure S3. The effect of incident wavelength. a, the beam shift varies as the incident wavelength changes in the range from 1710 nm to 1730 nm. **c**, the beam shift angle varies as the incident wavelength changes in the range from 1710 nm to 1730 nm. **b**, **d**, the intensity distribution at the wavelength of 1710 (**b**) and 1730 nm (**d**), respectively.

From the Fig. S3a, we observe that the beam shift in the X-direction exhibits greater variation compared to that in Y-direction, which is consistent with the results presented in the main text. The shift angle scans from 31.74° (at an incident wavelength

of 1710 nm) to 80.83° (at an incident wavelength of 1730 nm) as shown in Fig. S3c. Furthermore, the intensity distribution at an incident wavelength of 1710 nm is primarily concentrated in the first quadrant (Fig. S3b), while at an incident wavelength of 1730 nm, the intensity distribution shifts toward the Y-axis (Fig. S3d).

Therefore, by selecting an appropriate incident wavelength and considering the effect of refractive index changes on beam shifts, the beam shifts can be adjusted more flexibly to meet specific design requirements. As shown in Fig. S4, the refractive index range that is sensitive to beam shift angle variation will shift toward a higher values as the incident wavelength increase from 1720 nm to 1730 nm. Selecting a suitable incident wavelength allows for a greater shift angle scanning range while avoiding the influence of other modes. It is observed that at an incident wavelength of 1720 nm and a refractive index of 3.34, the intensity distribution becomes disordered due to interference from another Γ-BIC mode. This interference explains why the shift angle is notably low under these conditions.

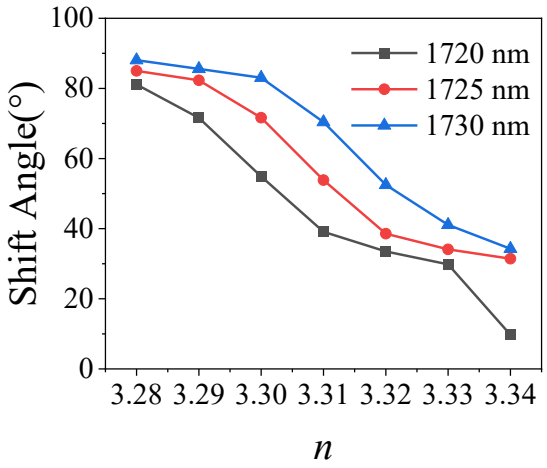

Figure S4. The effect of incident wavelength and refractive index. The shift angle at the incident wavelength of 1720 nm (black), 1725 nm (red) and 1730 nm (blue).

Section 4. The error caused by using different simulation methods.

In the main text, we applied the finite element method (FEM) to simulate the eigenmodes of a structure with infinite periodicity, while the finite-difference time-domain (FDTD) method was used to simulate the scattering characteristic of a real device with finite periodicity under specific incidence conditions. However, the use of these two different methods, along with their inherent inaccuracies, introduces errors that affect their output wavelength values. These errors cause the band structure to broaden and shift relative to the wavelength position. As shown in Fig. S5a-b. Compared to the result of band structure obtained by calculating the eigen mode using FEM (Fig. S5a), the band structure obtained by emission spectrum using FDTD method shifts relative to wavelength towards higher value. The impact of these discrepancies on beam shifts is more evident in Fig. S5c-d. The direction of beam shift at the wavelength of 1428 nm (purple line) calculated by FEM (Fig. S5c) is opposite to that obtained by using FDTD method (Fig. S5d).

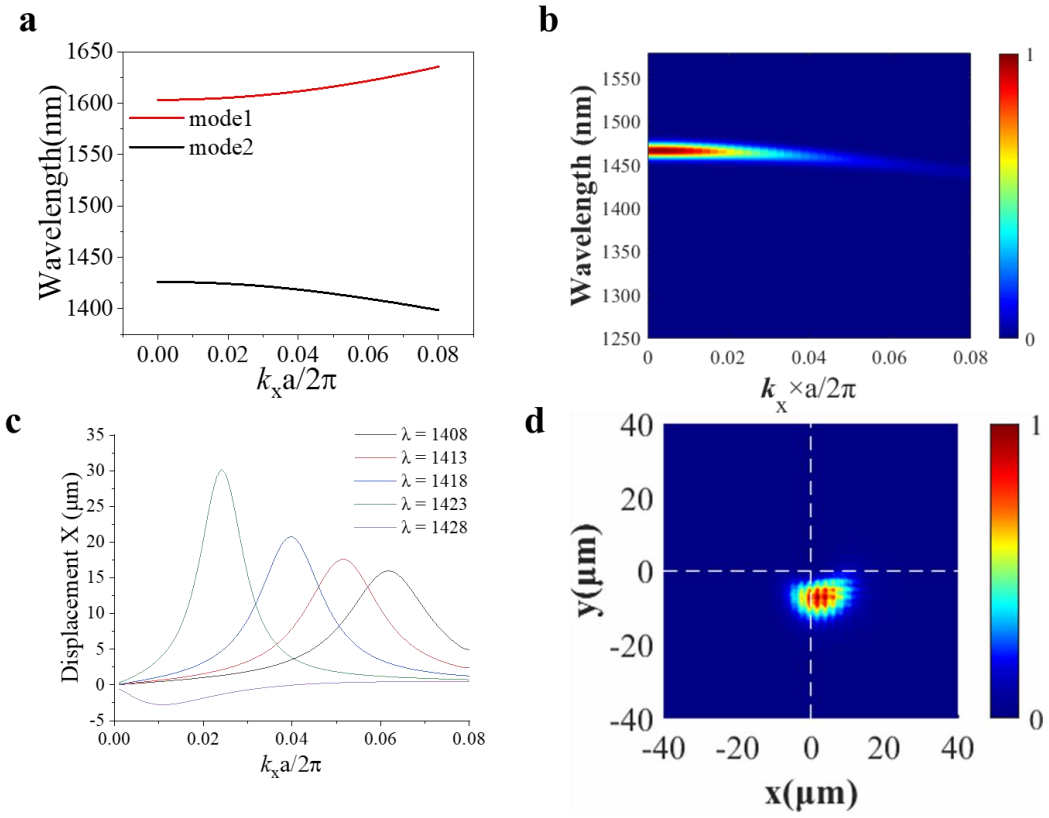

Figure S5. Comparison of simulation results using FEM and FDTD methods. a. The band structure of mode 2 calculated by FEM, represented by the black line. **b**. The band structure of mode 2 calculated by FDTD method, showing a shift relative to wavelength position compared to the FEM results. **c**. Beam shifts at different incident wavelength, the reflected light is approximately located on the Y-axis at an incident wavelength of 1428 nm. **d**. The reflected light is clearly located in the fourth quadrant at the same incident wavelength of 1428 nm.